The novel approach to spectral efficiency enhancement using massive MIMO in LoS

Nirav D. Patel, Vijay K. Patel

The novel approach to spectral efficiency enhancement using massive MIMO in LoS

Nirav D. Patel* and Vijay K. Patel

Faculty of Engineering and Technology,
Ganpat University,
384012, India
Email: nirav2009ec@gmail.com
Email: vijay.patel@ganpatuniversity.ac.in
*Corresponding author

Abstract: Future cellular wireless communication is likely to be shifted at mmWave band and results in large propagation loss. The loss can be reduced by shorter range and LoS type of communication. Focusing on futuristic scenario, the goal is to determine average sum Spectral Efficiency using OCM estimator and compare it with other estimators in LoS. Also Massive MIMO technology used to compensate for propagation loss along with the spatial multiplexing, beam forming, diversity gains. The multi-cell Massive MIMO system with maximum ratio transmit/receive precoding/combing method is considered. The obtained results are 26.09, 25.35, 24.56 and 15.18 bits/s/Hz/cell sum averaged UL SE and 26.80, 23.56, 23.14 and 15.06 bits/s/Hz/cell sum averaged DL SE using OCM, MMSE, EW-MMSE and LS estimators respectively. The OCM estimator outperform over other estimators. Also in general averaged sum spectral efficiency is increasing function of number of antennas at BS.

Keywords: only channel mean estimator; massive MIMO; spectral efficiency; mmWave band; minimum mean square error; element-wise minimum mean square error; least square error.

Biographical notes: Nirav D. Patel is an Electronics and Telecommunication Engineer with more than 12 years of achieving excellence in teaching, research, collaborating and contributing proactively to the academic environment. He has two published papers to his credit and has 12 years of academic, and three years of research experience. His research area includes wireless communications.

Vijay K. Patel completed his PhD in Wireless Communication in the year 2015. He is serving as an Associate Professor at Ganpat University – U V Patel College of Engineering, Gujarat, India. He is an Electronics and Telecommunications Engineer with more than 20 years of achieving excellence in teaching, research, consultancy, collaborating and contributing proactively to the academic environment. He played a significant role in the strategic development of the curriculum with experience of leading both undergraduate and graduate programs. He Served as Head of the Department of Electronics and Communications Engineering Department for more than 2 years. Currently, he is heading Information and Communication Technology Department. He successfully worked as an MTech {EC – VLSI and Embedded Systems} coordinator. He is selected as session Chair and delivered keynote speeches in various international conferences. He has published 18 research articles in the national and international journals. He has 22 years of academic, and five years of research experience. His research area includes wireless communications.

1 Introduction

Promising technologies are being investigated and integrated into the fifth generation (5G) and beyond mobile network systems. The main goal of these technologies is to overcome limitations of existing systems and to open up new dimensions to serve in better way. Some of the most pivotal key enabler technologies are millimetre Waves (mmWave), massive multiple input multiple output (MIMO), and small cells (SC) systems. These sets of technologies will dramatically increase the network throughput, enhance the spectral and energy efficiency, increase the network capacity and improve the network coverage by using the collaborative capabilities of the huge available bandwidth in mmWave frequencies while achieving high multiplexing gains through the extreme antenna arrays gains and achieving full coverage network by network densification through small cells (Mchangama et al., 2022; Ghosh et al., 2021). In this paper we present spectral efficiency analysis using massive MIMO in

millimeter wave band. Also small cells, channel estimation, beam forming technology, signal processing techniques are discussed in mmWave.

The launching of the commercial service for the fifth generation (5G) mobile network systems has been initiated since 2018 in many countries. 5G is the advanced bunch of technologies that will enable revolutionary applications not only in the telecommunication market but also, including industrial, automotive, medical, and even defense. The emerging technologies such as smart cities, smart homes, internet of things (IoT) are about to be a reality in near future. To serve this ever increasing demand of throughput, the research community has identified three ways to get several orders of magnitude throughput gain. Firstly, extreme densification of infrastructure. Secondly, large quantity of new bandwidth and finally, by integrating many more antennas, allowing throughput gain in the spatial dimension.

In order to face aforementioned problem, new technologies are emerging to make 5G and beyond networks to be able to meet the explosive demand of data rate. millimeter Wave (mmWave), MIMO and small cells (SCs) technologies are foreseen to be the answer of this high data demand (Mchangama et al., 2022). They are considered as the most promising technologies to leverage performance of 5G and beyond networks. 5G era is foreseen to lead in the next generation that will deliver ultra-high-speed connectivity, higher data rates with more robust reliability, higher spectral efficiency, lower energy consumption and wider coverage with high capacity than the legacy system.

Millimeter waves can provide a bandwidth of up to 252 GHz and the possibility of up to 100 GHz new spectrum for mobile applications (Hasan et al., 2019). The extreme high bandwidth in mmWaves makes it suitable for various applications in future networks such as front-hauling/back-hauling (Hasan et al., 2019), vehicular networks and forth. On the other hand, massive MIMO technology exploits spatial domain resources to offer diversity gain, multiplexing gain, and power gain (Björnson et al., 2017).

Likewise, small cells will offer thousands of connections and supported high transmission rate to provide variety local services (Hasan et al., 2019). Besides that, since small cells locate base stations near users, they are automatically one of the main drawbacks of mmWaves which is the high attenuation due to high frequencies with the distance. Moreover, small cells reduce the effect of blocking due to the need of going through walls.

1.1 MmWave

mmWave spectrum has been employed in different application such as in radars, satellite communication and point to point (PPT) communication application but not for commercial wireless networks. However, mmWave have recently appeared in short range communication (Hasan et al., 2019) and mobile broadband networks. About

28 GHz bandwidth is being identified for mmWave cellular networks while 57–64 GHz oxygen absorption band is excluded, and it is considered a best suited for indoor fixed wireless communication (Al-Ogaili and Shubair, 2016). The extreme high data rate in mmWave bands makes it adequate for different applications such as vehicular network and fronthauling/backhauling. Another advantage of mmWave is its small wavelength which makes it possible to design small antenna that can easily be integrated on chips. Furthermore, the relatively closer spectral allocation in mmWave bands leads to a more homogeneous propagation unlike the disjointed spectrum in precedent network. Besides that, mmWave communication is foreseen to be a best solution to replace fibre optics backhauling in areas where installation of fibre optics will be difficult (Mchangama et al., 2022). Additionally, narrow beams in mmWaves ease on packing more antenna elements.

Over the last three decades, various studies and measurements have been conducted in order to gain a deep knowledge of the special and temporal characteristics of millimeter wave frequency bands for the sake of developing new methods and techniques that will ease operating over mmWave bands, most of these studies and measurements were done in the 40 GHz band, 50 GHz band and 60 GHz band than at microwave bands (Mchangama et al., 2022). Recently in the 28 GHz, 38 GHz band and 72 GHz band, all of these were sub 100 GHz, however, currently the above 100 GHz gained high attention though it lacks measurements (Bansal et al., 2019; Hasan et al., 2019; Al-Ogaili and Shubair, 2016).

Despite the high bandwidth that mmWave can provide, it also suffers of atmospheric absorption, blockage effect such as human body blockage and self-blockage caused by on-chip components and human activities (Hasan et al., 2019; Al-Ogaili and Shubair, 2016; Abu-Rgheff, 2020).

Why mmWave:

1 *Large bandwidth*

With mmWave bands a peak data rate of about 10 Gbits/s can be achieved and this can increase with full duplex capability. This is much higher compared to 1 Gbits/s at low microwave frequencies (Mchangama et al., 2022; Ghosh et al., 2021).

2 *Short wavelength*

mmWave bands have a very small wavelength compared to currently used microwave bands. This makes them possible to have tiny size components, thus enabling integrating of more antennas in a small sized device, therefore, it will help to miniaturise physically smaller circuits, modules and equipment for 5G mmWave application (Mchangama et al., 2022; Ghosh et al., 2021). Another advantage of short wavelength is the high antenna gains. According to electromagnetic and antennas theories, shorter wavelength of mmWave can obtain proportionally higher antenna gains.

3   Narrow beams

In mmWave antennas arrays, highly directional steerable narrow beams can be formed to direct the transmit power precisely to the intended users along desired direction.

4   Increased security and interference immunity

The highly directional beams and greater resolution render mmWave signal difficult and costly to jam due to it is restricted to a relatively small area. In addition to that, narrow beams make mmWave transmission highly immune to interference and noise at the receiver side due to the ability to focus transmit power level of the signal.

1.2   Massive MIMO

Massive multiple-input multiple-output (MIMO) systems are state of art technology of current wireless systems. Prior MIMO systems, there were single-input single-output (SISO) system which was known of its low throughput, thus unable to support large number of users with highly reliability. This has led to the development of new MIMO systems such as the single user MIMO (SU-MIMO), multi-user MIMO (MU-MIMO) (Mchangama et al., 2022), however, these developed new MIMO systems could also not handle the ever-increasing demand of data. On top of that, the ongoing increase of connected devices and introducing of new application such as autonomous vehicles, smart cities, smart homes and more 5G applications, paved the integrating of new MIMO technologies that meet the requirements of 5G systems.

Massive MIMO technology is one of the most promising technologies in 5G and beyond networks systems. It is foreseen to be a powerful solution of massive data and connected devices related issues. Massive MIMO is a continuation of contemporary MIMO technology used in current networks which involves using hundreds or even thousands of antennas at the base station. The extreme use of antenna arrays in massive MIMO systems will leverage focusing energy into smaller regions of space which will provide better spectral efficiency and throughput.

Augmenting the numbers of antennas in a massive MIMO system makes the radiated beams narrow and spatially focused toward the user (Björnson et al., 2017), this increase the throughput for the intended user and mitigate the interference to neighbouring users.

1.3   Small cells

Small cells are known as miniature base stations that break up a cell site into much smaller pieces, they encompass Pico cells, Micro cells and Femto cells, they can comprise of indoor/outdoor system. The main goal of small cells is to increase the macro cells edge data capacity, speed and overall network performance. Small cells were firstly added in release 9 of the 3rd Generation Partnership Project (3GPP) LTE spec in 2012 (3GPP LTE Version 9.9.0, 2012) and they are one element of network densification. These small cells base stations (SCBs) will avail a short range communication to mobile terminals (MTs) to reduce propagation loss of signal transmission (Mchangama et al., 2022). By using mmWave and massive MIMO technologies, small cells can utilise large number of antennas to form directional beams to MT and provide concurrent transmission simultaneously.

Moreover, small cells deployment is considered to be an efficient approach to enhance spectral efficiency (Mchangama et al., 2022). On the other hand, with mmWave and massive MIMO technologies, small cells are foreseen to be used for backhauling, this can be the best replacement of high capacity wired based solutions which require a very costly investment in infrastructure (Mchangama et al., 2022). Similarly, small cells are considered to be a promising solution to replace fibre optic front hauling in environment that installation of fibre seem to be impossible (Mchangama et al., 2022).

1.4   Why LoS channel analysis

The current cellular wireless communication is mostly limited up to sub 6 GHz frequency range. However, data traffic expected to be increased 1000 times more in future compared to existing traffic (Bansal et al., 2019). To handle this tremendously increased wireless data traffic, the existing frequency spectrum up to sub 6 GHz is not capable. The shifting towards higher frequency spectrum ranging from sub 6 GHz to 100 GHz or sometime up to THz is the appropriate solution to handle future wireless data traffic, which have very large bandwidth and it will address the problem of congested data traffic at existing lower frequency band. However, the solution is not as simple as it looks. The mmWave (i.e., 30 GHz to 300 GHz) signal can have wavelength ranging from 10 mm to 1 mm, which is very small (Sun and Qi, 2019; Mihret et al., 2020). Such a small wavelength signal is more susceptible to free space path loss (FSPL), atmospheric attenuation (rain and hail), building penetration loss, blockage from obstacles, diffuse scattering from rough surface, shadowing and reflection losses (Hasan et al., 2019; Alouzi et al., 2021). The atmospheric attenuation due to oxygen absorption or heavy rain can be on the order of 10–20 dB/Km at frequency band ranging from 30 GHz to 300 GHz (Al-Ogaili and Shubair, 2016). The scattering losses are more due to having smaller wavelength, because scattering can be possible from roughness in order of wavelength. In short, signal losses are higher at mmWave band and non line of sight (NLoS) propagation has penetration, absorption, shadowing, reflection, refraction, and scattering losses at same mmWave band. However, mmWave technology has high data rate, low latency, and high bandwidth advantages over existing frequency band (i.e., Sub-6 GHz). Also the FSPL can be reduced in mmWave case by reducing distance between base station (BS) and user equipment (UE) using cell densification means given coverage area is covered by more cells compare to previous technology. As result, the distance between BS and UE is going to be reduced up to large extend and line of sight (LoS) is likely to be between

BS and UE. The LoS between BS and UE can reduce FSPL, penetration, absorption, shadowing, reflection, refraction, and scattering losses up to large extend.

In summary, future wireless communication will shift at mmWave band (above sub 6 GHz) for higher data rate, low latency and high band width using cell densification in same coverage area, which results in LoS between BS and UE.

2 Literature review

The 5G technology provide high data rate, low latency and high bandwidth compared to 4G technology using mmWave spectrum, so it is pivotal to model channel in mmWave band for next generation wireless standards (Zaman and Mowla, 2020; Carrera et al., 2020; Alouzi et al., 2021; Sun and Qi, 2019; Mihret et al., 2020; Bhuyan et al., 2019; Li et al., 2020). The penetration loss is higher at mmWave spectrum compared to microwave (Al-Ogaili and Shubair, 2016). On the other hand, the transceivers can pack large antenna arrays into small form factors at mmWave frequencies, making it possible to compensate the high path loss caused by high carrier frequency (Mihret et al., 2020). Also as per Du et al. (2021), the largest penetration loss is 16.068 dB at 144 GHz and the highest attenuation through clear glass is 27.633 dB/cm. As a result, it is desirable that the signal reach to the end without any type of blockage and it is possible by radiating sharp beam towards the UE directly, called beam forming gain. The beam forming gain and interference suppression can be achieved by Massive MIMO technology (Abu-Rgheff, 2020; Li et al., 2020; Carrera et al., 2020; Alouzi et al., 2021; Sun and Qi, 2019; Mihret et al., 2020; Rajmane and Sudha, 2019), which is key enabler technology in 5G. Also the LoS type of channel modelling is the most suitable for wireless communication at emerging mmWave technology (Karasawa, 2021). Hosany (2020) assumed perfect CSI for analysing spectral efficiency in 5G cellular network, however practically CSI is not available perfectly. Also, Hosany (2020) assumed the Rician channel fading model. However, in 5G with mmWave technology, the channel is almost LoS.

3 Core contribution

The limitations of prior works are majorly three. First, the channel models are assumed Rayleigh or Rician, however channels of 5G network with mmWave frequency are almost of LoS type. The large areas without obstructions, densification of small cells in given area, and unmanned vehicles serving from air (UAVs) are possible practical cases for such scenario (3GPP LTE Version 9.9.0, 2012). Second, usually the channel estimation required mean and channel covariance matrix statistics. However the LoS type channel required only the channel mean as a enough statistic for channel estimation, and there is no need of channel covariance matrix estimation. Third, the channel response is assumed to be change over coherent block, however channel is of LoS only type and the channel mean changes very

slowly compared to small scale fading coefficients. As result, channel estimation at every coherent block is not required and the computational complexity will reduce. In our research work this limited approach is tried to be broaden by below:

- considered multi-cell scenario with strong LoS between UE and its serving BS

- applied the only channel mean (OCM) estimator to estimate the LoS type channel and compared it with other Bayesian and non-Bayesian estimators

- sum average SE is determined for LoS type channels.

4 Channel and system modelling

In our research work, we have considered Massive MIMO system having hundreds of antennas at BS. Also the network is considered of L numbers of cells and each cell is assigned with dedicated single BS having M_j number of antennas. There are K number of UEs in each cell and each UE is equipped with single antenna. There is dedicated BS per cell to serve K number of UEs. The communication between BS and each UE is considered in time division duplex (TDD) mode, where channel responses are found constant over coherent slot and each coherent slot sized of τ_c samples. Also assumed independent channel realisation over every different coherent slot. The size of τ_c samples is determined by UE mobility and preoperational environment (Björnson et al., 2017). The coherent slot is divided into three types as per their utility. The τ_P samples for UL pilot signalling, τ_u samples for UL data transmission, and τ_d samples for DL data transmission, where $\tau_c = \tau_P + \tau_u + \tau_d$ (Björnson et al., 2017). In TDD mode, the channel reciprocity can be exploited for estimation of channel in UL using pilot signalling and assumed DL channel estimation same as UL. The $h_{lk}^j \in h^{M_j}$ is channel response of propagation, where subscript *l,* subscript *k* and superscript *j* indicates cell number, equipment number and BS number respectively. The each element of channel response vector represents propagation of signal from user equipment to any one of M_j antennas of BS. For notational convenience, h_{lk}^j used for UL channel and $(h_{lk}^j)^H$ used for DL channel, since there is no difference in channel response in UL and DL in same coherent slot.

In general the channel can be modelled as,

$$h_{lk}^j \sim \mathcal{N}_{\mathbb{C}} \left(\bar{h}_{lk}^j, R_{lk}^j \right), \tag{1}$$

where $\forall j,l \in 1,\ldots,L$ and $\forall k \in 1,\ldots,K$ and channel realisation assumed as the circularly symmetric complex Gaussian distributed (Björnson et al., 2017). In equation (1), the channel mean $\bar{h}_{lk}^j \in \mathbb{C}^{M_j}$ represents the LoS component and positive semi-definite covariance matrix $R_{lk}^j \in \mathbb{C}^{M_j \times M_j}$ represents to NLoS components with spatial correlation (Björnson et al., 2017). The Gaussian distribution describes

small-scale fading and macroscopic propagation effects represent the shadow fading, path loss, radiation patterns of antennas, which can be modelled by R_{lk}^j and $\bar{h}_{lk}^j$ (Patel and Patel, 2022). The average channel gain is obtained by taking trace of R_{lk}^j and normalised over M_j as

$$\beta_{lk}^j = \frac{1}{M_j} tr\left(R_{lk}^j\right), \tag{2}$$

is large scale fading coefficient.

5 Estimation methods

For receive processing channel state information is essential, which can be acquired by estimating the channel using τ_P pilot samples in each coherent slot in UL. The different orthogonal combinations of pilot sequence are possible and each orthogonal combination can be assigned to UE. The set of such orthogonal combinations can be reused in more than one cell with condition that the each user equipment within cell has unique pilot sequence. The $\varnothing_{jk} \in \mathbb{C}^{\tau_P}$ is deterministic pilot sequence, where $\varnothing_{jk}^2 = \tau_P$. Here pilot sequence set

$$p_{jk} = \left\{(l,i): \varnothing_{li} = \varnothing_{jk}, l=1,\ldots,L, i=1,\ldots,K_l\right\} \tag{3}$$

is the set of such sequences, which is used by user equipment k in every cell l and it is same as used by user equipment k in cell j. The pilot signal $Y_p^j \in \mathbb{C}^{M_j \times \tau_P}$ received at BS j is

$$Y_p^j = \sum_{k=1}^{K_j}\sqrt{P_{jk}}h_{jk}^j\varnothing_{jk}^T + \sum_{\substack{l=1 \\ l \neq j}}^{L}\sum_{i=1}^{K_l}\sqrt{P_{li}}h_{li}^j\varnothing_{li}^T + N_j^p, \tag{4}$$

where $N_j^p \in \mathbb{C}^{M_j \times \tau_P}$ has independent and identically distributed elements as $\mathcal{N}_\mathbb{C}\left(0,\sigma_{ul}^2\right)$. The BS j multiplies user equipment's pilot sequence $\varnothing_{li}^*$ with Y_p^j to obtain,

$$y_{jli}^p = Y_j^p\varnothing_{li}^* = \sqrt{P_{li}}\tau_P h_{li}^j + \sum_{(l',i')\in p_{li(l,i)}}\sqrt{P_{l'i'}}\tau_P h_{l'i'}^j + N_j^p\varnothing_{li}^* \tag{5}$$

for estimating channel h_{li}^j. The $y_{jli}^p \in \mathbb{C}^{M_j}$ can be used as statistic for estimating h_{li}^j sufficiently (Björnson et al., 2017). As per TDD protocol, channel is only estimated in UL and considered same in DL (Patel and Patel, 2022). However, if DL spectral efficiency is of interest, then data can be transmitted from BS and received at UE for spectral efficiency measurement.

The different channel estimators rely on statistical channel knowledge by different amount. There are three channel estimators have been considered here. The sample mean and sample covariance matrices can be used to estimate statistical distributions of channel (Björnson et al., 2017).

5.1 MMSE channel estimator

The MMSE estimation method can be applied by BS to acquire an estimation of h_{lk}^j by processing received pilot signal in equation (5) as per equation (6) shown below.

$$\hat{h}_{li}^j = \bar{h}_{li}^j + \sqrt{P_{li}}R_{li}^j\Psi_{li}^j\left(y_{jli}^p - \bar{y}_{jli}^p\right) \tag{6}$$

where $\hat{h}_{li}^j$ is channel estimation, $\bar{h}_{li}^j$ is channel mean, $\bar{y}_{jli}^p = \sum_{(l',i')\in p_{li}}\sqrt{P_{l'i'}}\tau_P\bar{h}_{l'i'}^j$ and

$$\Psi_{li}^j = \tau_P Cov\left\{y_{jli}^p\right\}^{-1} = \left(\sum_{(l',i')\in p_{li}}P_{l'i'}\tau_P R_{l'i'}^j + \sigma^2 I_{M_j}\right)^{-1} \tag{7}$$

It is noticeable here that, fully known statistical distribution required by Bayesian MMSE estimator. The covariance matrix of estimation error $\tilde{h}_{li}^j = h_{li}^j - \hat{h}_{li}^j$, is

$$C_{li}^j = R_{li}^j - P_{li}\tau_P R_{li}^j\Psi_{li}^j R_{li}^j \tag{8}$$

and trace of C_{li}^j is the mean square error, also defined as $\mathbb{E}\left\{h_{li}^j - \hat{h}_{li}^{j2}\right\}$. The MMSE estimate $\hat{h}_{li}^j$ and estimation error $\tilde{h}_{li}^j$ are distributed as

$$\hat{h}_{li,MMSE}^j \sim \mathcal{N}_\mathbb{C}\left(\bar{h}_{li}^j, R_{li}^j - C_{li}^j\right), \tag{9}$$

$$\tilde{h}_{li,MMSE}^j \sim \mathcal{N}_\mathbb{C}\left(0_M, C_{li}^j\right) \tag{10}$$

independent random variables, respectively. As per equations (8) and (10), it is noticeable that the mean value has no role over the estimation error covariance matrix. The estimation error does not affected by channel vector means as they are deterministic and can be filtered out while processing received signal. Moving ahead, as it is assumed that the channels are independent but in the set $\mathscr{p}_{li}$ the channel estimates of UEs are not independent. This is called pilot contamination, which occurs due to the same pilot sequence used by many UEs in different cells and the pilot reuse technique does not adhered finite pilot assignment constraint. The user equipment $(j, k) \in \mathscr{p}_{li}$ has the channel estimate

$$\hat{h}_{jk}^j = \bar{h}_{jk}^j + \sqrt{P_{jk}}R_{li}^j\Psi_{li}^j\left(y_{jli}^p - \bar{y}_{jli}^p\right) \tag{11}$$

and it is correlated with $\hat{h}_{lk}^j$ since y_{jli}^p common in both expressions and $\Psi_{li}^j = \Psi_{jk}^j$.

5.2 Element-Wise channel estimator

When entire covariance matrices does not known by BS, the MMSE estimation is not as effective as can be, due to the lake of statistical information. However in such case, the EW-MMSE estimation is optimum option and can be a substitute of MMSE estimation (Patel and Patel, 2022). The

diagonal elements of covariance matrices are only been estimated independently by EW-MMSE estimation method. As a result, EW-MMSE is more simplex compared to MMSE in terms of computational complexity, since matrix inversions are not required. The channel estimation by EW-MMSE is defined as

$$\hat{h}_{li}^{j} = \overline{h}_{li}^{j} + \sqrt{P_{li}} D_{li}^{j} \Lambda_{li}^{j} \left(y_{jli}^{p} - \overline{y}_{jli}^{p} \right), \tag{12}$$

where $D_{li}^{j} \in \mathbb{C}^{M_j \times M_j}$ and $\Lambda_{li}^{j} \in \mathbb{C}^{M_j \times M_j}$ are diagonal matrices with $D_{li}^{j} = diag\left(\left[R_{li}^{j} \right]_{mm} : m = 1 \ldots M_j \right)$ and

$$\Lambda_{li}^{j} = diag\left(\left[\sum_{(l',i) \in p_{li}} P_{l'i} \tau_P R_{l'i}^{j} + \sigma^2 I_{M_j} \right]_{mm} : m = 1 \ldots M_j \right)^{-1}.$$

The EW-MMSE estimate $\hat{h}_{li}^{j}$ and estimation error $\tilde{h}_{li}^{j}$ are correlated and distributed as

$$\hat{h}_{li,EW-MMSE}^{j} \sim \mathcal{N}_{\mathbb{C}} \left(\overline{h}_{li}^{j}, \Sigma_{li}^{j} \right) \tag{13}$$

$$\tilde{h}_{li,EW-MMSE}^{j} \sim \mathcal{N}_{\mathbb{C}} \left(0_M, \tilde{\Sigma}_{li}^{j} \right) \tag{14}$$

respectively, where $\Sigma_{li}^{j} = P_{li} \tau_p D_{li}^{j} \Lambda_{li}^{j} (\Psi_{li}^{j})^{-1} \Lambda_{li}^{j} D_{li}^{j}$ and $\tilde{\Sigma}_{li}^{j} = P_{li} \tau_p R_{li}^{j} \Lambda_{li}^{j} D_{li}^{j} - P_{li} \tau_p D_{li}^{j} \Lambda_{li}^{j} R_{li}^{j} + \Sigma_{li}^{j}$.

Here in EW-MMSE estimation, desired results can be achieved same way as MMSE estimation, but estimation of every single element is carried out by processing signal received at each antenna and statistics are computed as result (Patel and Patel, 2022). It is noticeable that if covariance matrices have none zero diagonal elements and zero off diagonal elements then there is same performance result of EW-MMSE as it can be with MMSE. In such cases EW-MMSE estimation is optimal choice, as less computational efforts required than MMSE estimation.

5.3 LS channel estimator

When there is no prior information available (regarding R_{li}^{j} and $\overline{h}_{li}^{j}$), estimation by non Bayesian estimator is suitable substitute over Bayesian estimators. The LS estimation is one of these kinds of estimation methods by which h_{li}^{j} channel can be estimated during propagation (Patel and Patel, 2022). The value of $\hat{h}_{li}^{j}$, which minimises $y_{jli}^{p} - \sqrt{P_{li}} \tau_P \hat{h}_{li}^{j2}$, is called LS estimator. Which can be expressed as

$$\hat{h}_{li}^{j} = \frac{1}{\sqrt{P_{li}} \tau_P} y_{jli}^{p}, \tag{15}$$

where distribution of $\hat{h}_{li}^{j}$ and $\tilde{h}_{li}^{j}$ is defined as

$$\hat{h}_{li,LS}^{j} = \mathcal{N}_{\mathbb{C}} \left(\frac{1}{\sqrt{P_{li}} \tau_P} \overline{y}_{jli}^{p}, \frac{1}{P_{li} \tau_P} \Psi_{li}^{j-1} \right), \tag{16}$$

$$\tilde{h}_{li,LS}^{j} = \mathcal{N}_{\mathbb{C}} \left(\overline{h}_{li}^{j} - \frac{1}{\sqrt{P_{li}} \tau_P} \overline{y}_{jli}^{p}, \frac{1}{P_{li} \tau_P} \Psi_{li}^{j-1} - R_{li}^{j} \right) \tag{17}$$

respectively. The $\hat{h}_{li}^{j}$ and $\tilde{h}_{li}^{j}$ are estimation and estimation error of channel respectively, which are correlated random variables.

As it is noticeable, LS channel estimation is simple and less computationally complex than other two methods, but LS estimation has to pay for that by having channel estimation statistics more complex than MMSE and EW-MMSE estimators. This can be seen in above equation (17) as non-zero mean in estimation error and it is compromise in communication performance

5.4 Only mean channel (OMC) estimator

If only the mean values of the UE's channel are known by BS and covariance matrices are not known, then only mean values can be used for channel estimation, called only mean channel (OMC) estimator. The mean values variation is very small compared to the small-scale fading coefficients and does not need to be estimate in each coherent slot. As a result, it does not required to send pilot in each coherent slot for channel estimation. Thus, the computational complexity reduce extensively since the channels are not required to estimate in each coherent slot. However, OCM estimator is meaningless without having LoS path since it ignores the NLoS paths. So if strong LoS path does not exist in given scenario then OCM estimator does fail.

6 Up-link and down-link spectral efficiency

The received signal $y_j \in \mathbb{C}^{M_j}$ at BS j, during data transmission, is

$$y_j = \sum_{k=1}^{K_j} h_{jk}^{j} s_{jk} + \sum_{\substack{l=1 \\ l \neq j}}^{L} \sum_{i=1}^{K_l} h_{li}^{j} s_{li} + n_j \tag{18}$$

where additive noise is defined as $n_j \sim (0_{M_j}, \sigma^2 I_{M_j})$. The $s_{lk} \in \mathbb{C}$ is the UL signal in cell l from user equipment k and $p_{lk} = \mathbb{E}\{s_{lk}^{2}\}$ is power of s_{lk}. In equation (18) first term is desired signal; second term is interference and last term is noise. The receive combining vector $v_{jk} \in \mathbb{C}^{M_j}$ is selected by BS j to multiply with y_j to separate out interference from desired signal coming from user equipment k, where v_{jk} is selected based on CSI available at BS. In Björnson et al. (2017), the UL capacity (ergodic) is lower bounded by

$$SE_{jk}^{ul} = \frac{\tau_u}{\tau_c} \log_2 \left(1 + \gamma_{jk}^{ul} \right) \text{ bits/s/Hz} \tag{19}$$

where γ_{jk}^{ul} is effective SINR expressed as,

$$\gamma_{jk}^{ul} = \frac{p_{jk}\left|\mathbb{E}\{\mathbf{v}_{jk}^{H}h_{jk}^{j}\}\right|^{2}}{\sum_{l=1}^{L}\sum_{i=1}^{K_{l}}p_{li}\mathbb{E}\left\{\left|\mathbf{v}_{jk}^{H}h_{li}^{j}\right|^{2}\right\} - p_{jk}\left|\mathbb{E}\{\mathbf{v}_{jk}^{H}h_{jk}^{j}\}\right|^{2} + \sigma_{ul}^{2}\mathbb{E}\{\mathbf{v}_{jk}^{2}\}}$$

(20)

where expectation is carried out from all sources of randomness in equation (20). The SE in equation (19) is ergodic achievable SE as it is below the capacity.

The reverse process can be followed for Down-Link (DL) spectral efficiency measurement. In which, data signal is transmitted from BS and received at UE. Here it is noticeable that the channel is estimated only in UL and considered same in downlink as per TTD protocol. The closed form equations of DL SE and SINR can be derived and followed for analysis.

However, the UL SE SE_{jk}^{ul} and SINR γ_{jk}^{ul} can be achieved using MR combing, where for MMSE and EW-MMSE estimators the MR combing vector is $v_{jk} = \hat{h}_{jk}^{j}$ in UL, for OCM estimator the MR combing vector is $\mathbf{v}_{jk} = \bar{h}_{jk}^{j}$ and for LS estimator the MR combing vector is $\mathbf{v}_{jk} = \frac{1}{\sqrt{p_{jk}\tau_{p}}}y_{jjk}^{p}$. The DL SE SE_{jk}^{dl} and SINR γ_{jk}^{dl} can be achieved using MR precoding, where for MMSE, EW-MMSE and LS estimators the MR precoding vector is $w_{lk} = \frac{\hat{h}_{jk}^{j}}{\sqrt{\mathbb{E}\{\hat{h}_{jk}^{j\,2}\}}}$ and for OCM estimator the MR precoding vector is $w_{lk} = \frac{\bar{h}_{jk}^{j}}{\bar{h}_{jk}^{j}}$.

7 Basic setup and configuration

The Setup assumed and configured as there are 16 cells and each cell has 62500 m² (250 × 250 m) square shape area with wrap around topology, such that this layout ensure substantially equal interference to each BS from every direction. The UEs are assumed 10 per cell, which are distributed independently and uniformly in each cell at least 35 m away from BS. The user equipment assignment to the single BS among possible BSs options is carried out by ensuring largest channel gain availability to that BS. The large scale fading and nominal angle are computed as per user equipment locations.

The uniformly half wave-length spaced and linearly distributed (ULA) antennas are considered at each BS. The direct propagation component is defined as (Björnson et al., 2017),

$$\bar{h}_{li}^{j} = \sqrt{\beta_{li}^{j,LoS}}\,[1\ e^{j2\pi d_{H}\sin(\varphi_{li}^{j})}\ \dots\ e^{j2\pi d_{H}(M-1)\sin(\varphi_{li}^{j})}]^{T}$$

(21)

where the $\beta_{lk}^{j,LoS}$ is the co-efficient of large scale fading, $d_{H} \leq \frac{\lambda}{2}$ is the spacing between antennas, and φ_{lk}^{j} is the angle of arrival (AoA). In equation (21), the co-efficient of

large scale fading is $\beta_{lk}^{j,LoS} = \frac{1}{M_{j}}\bar{h}_{li}^{j2}$, which is finite value for any M_{j}. The number of scattering clusters N is considered 6 for covariance matrices and it is approximately modelled as

$$\left[R_{li}^{j}\right]_{s,m} = \frac{\beta_{li}^{j,NLoS}}{N}\sum_{n=1}^{N}e^{j\pi(s-m)\sin(\varphi_{li,n}^{j})}e^{-\frac{\sigma_{\varphi}^{2}}{2}\left(\pi(s-m)\cos(\varphi_{li,n}^{j})\right)^{2}}$$

(22)

where $\beta_{lk}^{j,NLoS}$ is the large scale fading co-efficient for non direct paths, $\varphi_{li,n}^{j} \sim \mathcal{U}\left[\varphi_{li}^{j}-40°,\varphi_{li}^{j}+40°\right]$ is the nominal angle of arrival (Patel and Patel, 2022), where n is the number of clusters, s is row number and m is column number of R_{li}^{j}. Here the Gaussian local scattering model (Björnson et al., 2017) is considered for the covariance matrix $\left[R_{li}^{j}\right]_{s,m}$ of each cluster. The Gaussian distributed angle of arrivals of multipath components of a cluster are distributed with the ASD (Angular Standard Deviation) $\sigma_{\varphi} = 5°$ around the nominal angel of arrival (Özdogan et al., 2019). The channel bandwidth for communication is considered 200 MHz (3GPP, 2019; 5G Americas White Paper, 2020) and the total receive noise power is considered −94 dBm (Özdogan et al., 2019). The samples per each coherence slot are considered 200 and the pilots in each cell (one per user equipment) are considered 10 (Björnson et al., 2017). The pilot assignment to the UEs is random in each cell such that the kth UEs in two or more cells belonging to same pilot group have same pilot assignment.

Also, it is assumed that there are always dominant LoS paths available between UE and BS pairs and the large scale fading coefficient in presence of LoS paths, is modelled (in dB) as (3GPP, 2020)

$$\beta_{li}^{j} = -30.18 - 26\log_{10}\left(d_{li}^{j}\right) + F_{li}^{j},$$

(23)

where $F_{li}^{j} \sim \mathcal{N}(0,\ \sigma_{sf}^{2})$ is shadow fading with $\sigma_{sf} = 4$ (3GPP, 2020). The formula for Rician factor is $k_{li}^{j} = 13 - 0.03d_{li}^{j}$ [dB] (Özdogan et al., 2019). The large scale fading parameters in terms of large scale fading coefficient β_{li}^{j} and Rician factor k_{li}^{j} are defined as (3GPP, 2020)(3GPP, 2020)(3GPP, 2020)

$$\beta_{li}^{j,LoS} = \sqrt{\frac{k_{li}^{j}}{k_{li}^{j}+1}}\beta_{li}^{j}\ \text{and}\ \beta_{li}^{j,NLoS} = \sqrt{\frac{1}{k_{li}^{j}+1}}\beta_{li}^{j}$$

(24)

For optimum power allocation, the UL power control policy decided by heuristic approach as (Björnson et al., 2017)

$$p_{jk} = \begin{cases} p_{max}^{ul}, & \Delta > \frac{\beta_{jk}^{j}}{\beta_{j,min}^{j}}, \\ p_{max}^{ul}\Delta\frac{\beta_{j,min}^{j}}{\beta_{jk}^{j}}, & \Delta \leq \frac{\beta_{jk}^{j}}{\beta_{j,min}^{j}}, \end{cases}$$

(25)

where p_{jk} is the transmit power. The p_{max}^{ul} is maximum UL power with value 10 dBm and minimum large scale fading

coefficient defined as $\beta_{j,min}^{j} = \min(\beta_{j1}^{j}, \ldots \beta_{jk}^{j} \ldots, \beta_{jK}^{j})$. The policy allows the weakest channel user equipment with full power and reduces power of the remaining UEs such that their UL SNRs are not more than $\Delta = 10$ dB higher. The power received by user equipment ρ_{jk} considered same as power transmitted by user equipment p_{jk} for simplicity. So above equation (25) can be applicable for DL SE measurement also with just notational change.

8 Output results

In this section, validation and evaluation of close form expressions for Massive MIMO cellular networks is carried out by simulation.

Figure 1 provides plots of average sum UL SE for various numbers of BS antennas, averaged over number of realisation of various shadow fading and user equipment locations. Also the MR combing method has been chosen for receive combing. The propagation scenario has been assumed as having LoS path between all UE-BS pairs and also assumed spatially correlated Rician fading channel between every pair UE-BS. Further, the averaged sum UL SE has been determined as a function of number of BS antennas, using OCM, MMSE, EW-MMSE and LS estimators. The SE curves are plotted for each estimation method for comparative analysis. The square marker plots are carried out using Monte-Carlo simulation and remaining plots are carried out using expressions available above, called analytical method. The alignment of Monte-Carlo curves with analytical curves is validating our results. The

results reveal that UL SE is increasing function of number of BS antennas for any estimation method. However, the SE using OCM estimator is highest among all and SE is decreasing for remaining estimators in order of MMSE to EW-MMSE to LS estimators. Also the performance gap between LS and remaining estimators is large and it is getting increased with increase in BS antennas.

The numerical values of sum averaged UL SEs are 26.09, 25.35, 24.56 and 15.18 bits/s/Hz/cell for 100 BS antennas using OCM, MMSE, EW-MMSE and LS estimators respectively. Comparing the case where only some UE-BS pairs have LoS paths, the SE is higher here in the case where every UE-BS pair has LoS path, because the existence of LoS component improves SE. In summary, for special case of having LoS path between every UE-BS pair, the OCM estimator outperform over all other estimators.

Figure 2 provide plots of average sum DL SE for various numbers of BS antennas, averaged over number of realisation of various shadow fading and user equipment locations. Also the MR precoding method has been chosen for transmit precoding. The remaining all assumptions, configurations and descriptions are same as UL SE case (Figure 1). The results reveal that the DL SE is increasing function of number of BS antennas for any estimation method. Also in DL, the SE using OCM estimator is highest among all and SE is decreasing for remaining estimators in order of MMSE to EW-MMSE to LS estimators. The performance gap between LS and remaining estimators is large and it is getting increased with increase in BS antennas.

Figure 1 Average sum UL SE vs. no. of BS antennas when all UE-BS pairs have a LoS path in between and $k = 10$ (see online version for colours)
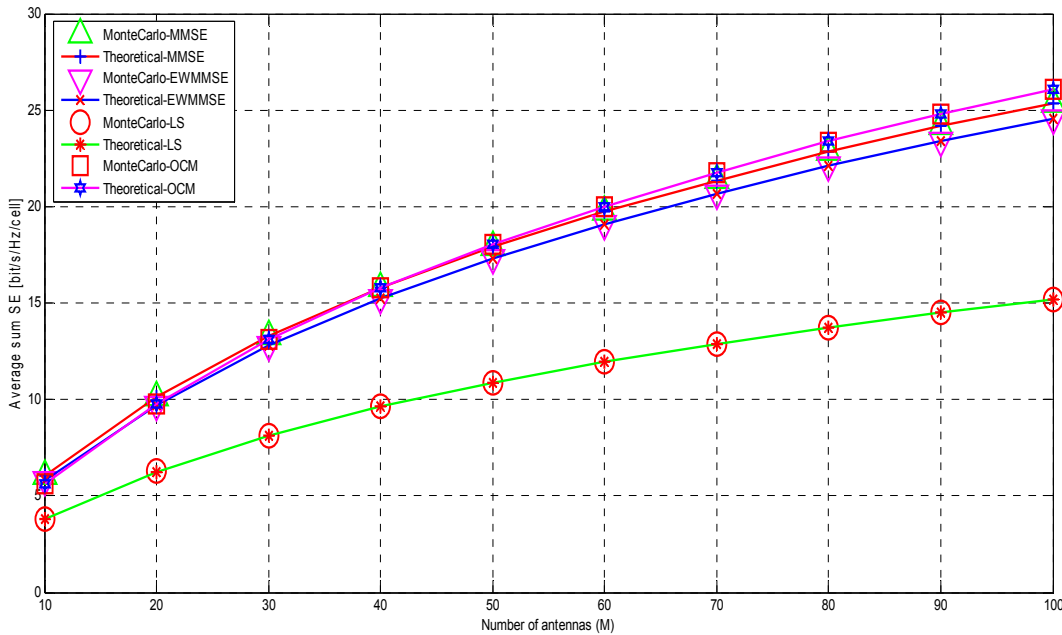
Figure 2   Average sum DL SE vs. no. of BS antennas when all UE-BS pairs have a LoS path in between and $k = 10$ (see online version for colours)
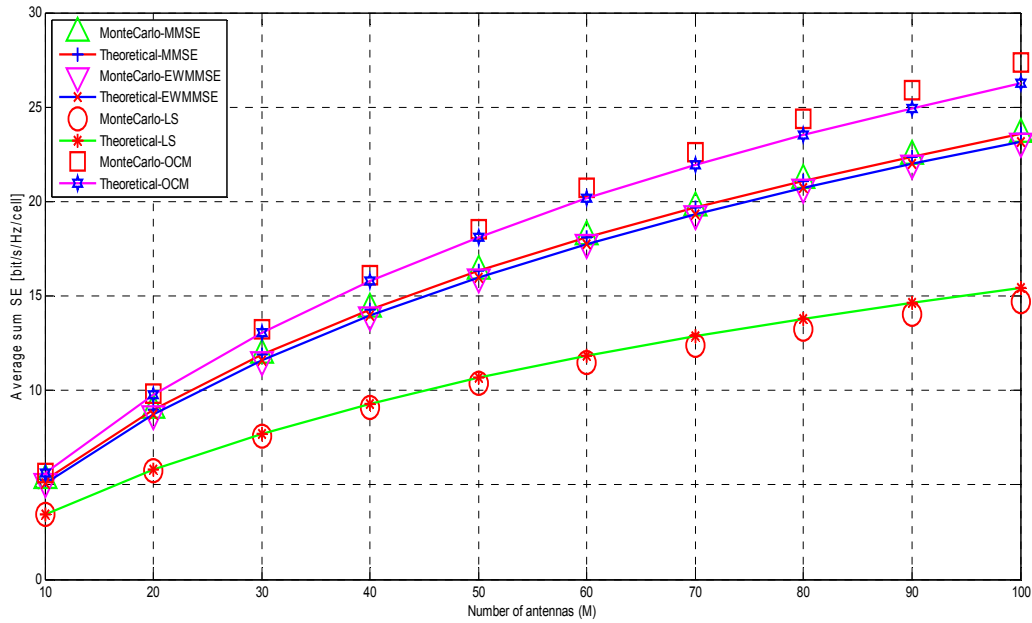
The numerical values of sum averaged UL SEs are 26.80, 23.56, 23.14 and 15.06 bits/s/Hz/cell for 100 BS antennas using OCM, MMSE, EW-MMSE and LS estimators respectively. Comparing the case where only some UE-BS pairs have LoS paths, the SE is higher here in the case where every UE-BS pair has LoS path, because the existence of LoS component improves SE. In summary, for special case of having LoS path between every UE-BS pair, the OCM estimator outperform over all other estimators in DL also.

9   Conclusion

Future wireless communication will be shifted at mmWave frequency spectrum, which increases signal attenuation and absorption. The short distance and LoS types of communication can reduce signal loss. So LoS type of propagation scenario is most suitable and likely to be scenario in future mmWave communication and our research work has focused on it.

The averaged sum UL and DL SE as function of number of BS antennas for the Massive MIMO system has be discussed, where every UE-BS pair has LoS path in between. The comparative analysis has been carried out for OCM, MMSE, EW-MMSE and LS estimators for UL and DL sum averaged SE. The results reveal that the SE is increasing function of number of BS antennas using any estimation method in UL and DL. Also the OCM estimator outperforms over all other estimators in both UL and DL cases. The SE is decreasing for remaining estimators in order of MMSE-to-EW-MMSE-to-LS. Comparing the SE for the case where the some UE-BS pairs have LoS paths, the SE is higher in case of all UE-BS pairs have LoS paths, which reveals that the existence of LoS components

improves SE. In summary, OCM estimator outperforms over other estimators when there are LoS paths existed between every pair of UE-BS in the system.

However, if there is Rayleigh fading existed between any pair of UE and BS and OCM estimator is used, then SE would become zero, which is the limitation of OCM estimator and should not be used for all kind of propagation scenarios.

References

3GPP LTE Version 9.9.0 (2012) 3GPP ETSI TS 136300 36.300 version 9.9.0 Release 9, 2012-01, LTE; Evolved Universal Terrestrial Radio Access (E-UTRA) and Evolved Universal Terrestrial Radio Access Network (E-UTRAN); Overall description; Stage 2.

3rd Generation Partnership Project (3GPP) (2019) *Technical Specification Group Services and System Aspects; Release 15 Description; Summary of Rel-15 Work Items (Release 15)*, 3GPP TR 21.915V15.0.0, September, 2019.

3rd Generation Partnership Project (3GPP) (2020) *Technical Specification Group Radio Access Network; Spatial Channel Model for Multiple Input Multiple Output (MIMO) Simulations (Release 16)*, 3GPP TR 25.996 V16.0.0 (2020-07), July 2020.

5G Americas White Paper (2020) *Understanding mmWave Spectrum for 5G Networks*, 5G Americas White Paper, December.

Abu-Rgheff, M.A. (2020) *5G Physical Layer Technologies*, John Wiley & Sons, Inc., Hoboken, NJ, USA.

Al-Ogaili, F. and Shubair, R.M. (2016) 'Millimeter-wave mobile communications for 5G: challenges and opportunities', *International Symposium on Antennas and Propagation (APSURSI)*, IEEE, Fajardo, PR, USA.

Alouzi, M., Chan, F. and D'Amours, C. (2021) 'Low complexity hybrid precoding and combining for millimeter wave systems', *IEEE Access*, IEEE, Vol. 9, pp.95911–95924.

Bansal, B., Mishra, V.K., Soni, S. and Jain, N. (2019) 'Deterministic millimeter-wave channel modeling based on ray-tracing in urban scenario', *International Conference on Signal Processing and Communication (ICSC)*, IEEE, Noida, India.

Bhuyan, A., Guvenc, I., Dai, H., Yapici, Y., Rahmati, A. and Maeng, S.J. (2019) 'Secure mmWave cellular network for drone communication', *IEEE 90th Vehicular Technology Conference (VTC2019-Fall)*, IEEE, Honolulu, HI, USA.

Björnson, E., Hoydis, J. and Sanguinetti, L. (2017) 'Massive MIMO networks: spectral, energy, and hardware efficiency', *Foundations and Trends® in Signal Processing*, Vol. 11, Nos. 3–4, pp.154–655.

Carrera, D.F., Vargas-Rosales, C., Villalpando-Hernandez, R. and Alejan, J. (2020) 'Performance improvement for multi-user millimeter-wave massive MIMO systems', *IEEE Access*, IEEE, Vol. 8, pp.87735–87748.

Du, K., Ozdemir, O., Erden, F. and Guvenc, I. (2021) 'Sub-terahertz and mmWave penetration loss measurements for indoor environments', *International Conference on Communications Workshops (ICC Workshops)*, IEEE, Montreal, QC, Canada.

Ghosh, J., Zhu, H. and Haci, H. (2021) 'A novel channel model and optimal beam tracking schemes for mobile millimeter-wave massive MIMO communications', *IEEE Transactions on Vehicular Technology*, IEEE, Vol. 70, No. 7, pp.7205–7210.

Hasan, R., Mowla, M.M., Rashid, M.A., Hosain, M.K. and Ahmad, I. (2019) 'A statistical analysis of channel modeling for 5G mmWave communications', *International Conference on Electrical, Computer and Communication Engineering (ECCE)*, IEEE, Cox's Bazar, Bangladesh.

Hosany, M.A. (2020) 'Efficiency analysis of massive MIMO systems for 5G cellular networks under perfect CSI', *3rd International Conference on Emerging Trends in Electrical, Electronic and Communications Engineering (ELECOM)*, IEEE, Balaclava, Mauritius.

Karasawa, Y. (2021) 'A multi state channel model composed of line-of-sight and semi-line-of-sight propagation environments for millimeter-wave mobile radio systems', *Transactions on Antennas and Propagation*, IEEE, Vol. 69, No. 12, pp.8731–8743.

Li, Y-N.R., Gao, B., Zhang, X. and Huang, K. (2020) 'Beam management in millimeter-wave communications for 5G and beyond', *IEEE Access*, IEEE, Vol. 8, pp.13282–13293.

Mchangama, A., Ayadi, J., Gil Jiménez, V.P. and Consoli, A. (2022) 'MmWave massive MIMO small cells for 5G and beyond mobile networks: an overview', *12th International Symposium on Communication Systems, Networks and Digital Signal Processing (CSNDSP)*, Porto, Portugal, IEEE.

Mihret, F., Kumar, P. and Srinivas, T. (2020) 'Hybrid photonic beamforming for 5G downlink millimeter wave MIMO communication', *IEEE International Conference on Electronics, Computing and Communication Technologies (CONECCT)*, Bangalore, India, IEEE.

Özdogan, Ö. and Björnson, Larsson, E.G. (2019) 'Massive MIMO with spatially correlated rician fading channels', *IEEE Transactions on Communications*, Vol. 67, No. 5, May, pp.3234–3250.

Patel, N.D. and Patel, V.K. (2022) 'The novel approach of down-link spectral efficiency enhancement using massive MIMO in correlated Rician fading scenario', *International Conference on Computing Science, Communication and Security (COMS2-1604)*, Springer, Cham, pp.54–68.

Rajmane, R.S. and Sudha, V. (2019) 'Spectral efficiency improvement in massive MIMO systems', *TEQIP III Sponsored International Conference on Microwave Integrated Circuits, Photonics and Wireless Networks (IMICPW)*, Tiruchirappalli, India, IEEE.

Sun, X. and Qi, C. (2019) 'Multiuser beam allocation for millimeter wave massive MIMO systems', *IEEE International Conference on Communications (ICC)*, IEEE, Shanghai, China.

Zaman, K. and Mowla, M.M. (2020) 'A millimeter wave channel modeling with spatial consistency in 5G systems', *Region 10 Symposium (TENSYMP)*, IEEE, Dhaka, Bangladesh.